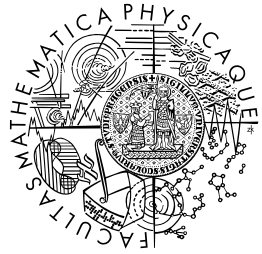

FACULTY
OF MATHEMATICS
AND PHYSICS
Charles University

Multipoint Observations of Magnetospheric Wave Phenomena

(Abstract of the Doctoral Thesis)

Barbora Bezděková

Department of Surface and Plasma Science

Supervisor of the doctoral thesis: doc. RNDr. František Němec, Ph.D.
Study programme: Physics
Study branch: Physics of Plasmas and Ionized Media

Prague 2020

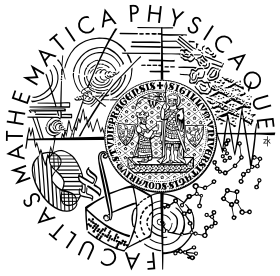

MATEMATICKO-FYZIKÁLNÍ
FAKULTA
Univerzita Karlova

Vícebodová pozorování magnetosférických vlnových jevů

(Autoreferát disertační práce)

Barbora Bezděková

Katedra fyziky povrchů a plazmatu

Školitel: doc. RNDr. František Němec, Ph.D.

Studijní program: Fyzika

Studijní obor: Fyzika plazmatu a ionizovaných prostředí

Praha 2020

Disertační práce byla vypracována na základě výsledků vědecké práce na Katedře fyziky povrchů a plazmatu v letech 2017–2020 během mého doktorského studia na Matematicko-fyzikální fakultě Univerzity Karlovy.

Uchazeč:
Mgr. et Mgr. Barbora Bezděková
Katedra fyziky povrchů a plazmatu, MFF UK
V Holešovičkách 2
180 00 Praha 8

Školitel:
doc. RNDr. František Němec, Ph.D.
Katedra fyziky povrchů a plazmatu, MFF UK
V Holešovičkách 2
180 00 Praha 8

Oponenti:
Ing. Benjamin Grison, Ph.D.
Ústav fyziky atmosféry, AV ČR
Boční II 1401
141 00 Praha 4

prof. David R. Shklyar
Institut Kosmicheskikh Issledovaniy
Ulitsa Profsoyuznaya 84/32
Moskva 117997
Rusko

Obhajoba se koná dne 11.12.2020 v 9.30 hodin před komisí pro obhajoby doktorských prací v oboru 4F2 Fyzika plazmatu a ionizovaných prostředí na MFF UK V Holešovičkách 2, 180 00 Praha 8, v místnosti č. 042.

S disertační prací je možné se seznámit na Studijním oddělení pro doktorské studium MFF UK, Ke Karlovu 3, 121 16 Praha 2.

Předseda RDSO 4F2: doc. RNDr. Jiří Pavlů, Ph.D.

Contents

Introduction

It has been commonly believed that a majority of the visible matter (99.9%) is formed by plasma, the so-called fourth fundamental state of matter. Although this state of matter might seem a little exotic, the truth is that basically the whole Earth is surrounded by plasma. This medium forms, among others, the Earth's magnetosphere. The magnetosphere of the Earth is a various, dynamic, and nearly collisionless system where many phenomena occur. One of the most significant phenomena are electromagnetic waves, which mediate the energy transfer in the environment without collisions.

Electromagnetic waves present in the Earth's magnetosphere which can be found basically everywhere are called whistler mode waves. Whistler mode waves occur in the frequency range below the characteristic frequencies (electron plasma and cyclotron frequencies) of the system and they represent one of the best and longest known class of the waves in plasma. Among others, whistlers, electromagnetic waves generated by lightning, are of the whistler mode and the whole wave class was named after them.

Although many of the whistler mode waves have already been known for decades, the origin of plenty of them is still not sufficiently understood. However, due to their undisputed importance for the Earth's magnetospheric dynamics, the whistler mode waves represent one of the leading research fields of the magnetospheric physics. The present thesis is focused on the analysis of two specific whistler mode wave types.

The first of them, quasiperiodic (QP) emissions, is currently intensively studied and observable basically by every suitable instrument. The events were initially described and classified already in the 1960's, but the latest observations still keep bringing new pieces of evidence, knowledge, and understanding.

The second investigated wave type, magnetospheric line radiation (MLR), is, in some sense, even stranger. Although originally regarded as of a possibly anthropogenic origin, they were recently shown to be a natural phenomenon. Moreover, according to the author's knowledge, no theoretical model of their generation has ever been developed.

In this thesis, conjugate observations of quasiperiodic emissions, magnetospheric line radiation properties, and a possible relation between both event types are studied. Moreover, a study of the variations of the overall wave activity during the periods around the interplanetary shock arrivals is presented.

Studied Wave Phenomena

Whistler mode waves, which occur in the very low frequency (VLF) range (3 Hz–30 kHz), are frequently observed in the Earth's magnetosphere. They were detected in all magnetospheric regions and they are of various kinds. It is generally assumed that the wave phenomena interact not only with plasma particles, but also with other wave events. However, to be able to describe concrete realizations of such interactions, a deep understanding of the behavior of individual wave types is desirable. In many cases, current knowledge of the wave phenomena is insufficient.

Magnetospheric Line Radiation

Whistler mode electromagnetic waves observed in the inner magnetosphere which are periodically modulated in the frequency domain are called magnetospheric line radiation. These events typically occur in the frequency range from about 1 to 8 kHz. Although the first observations of MLR events were performed by ground-based stations in Antarctica already in 70's [Helliwell *et al.*, 1975], their origin is not clear. During the years, MLR events were observed by both spacecraft [e.g., Bell *et al.*, 1982; Parrot *et al.*, 2005] and ground-based stations [e.g., Rodger *et al.*, 1999, 2000b], and also in conjugate regions [Helliwell *et al.*, 1975]. In frequency-time spectrograms, they can be easily identified as several almost parallel and nearly horizontal intense lines. An example of a frequency-time spectrogram measured by the French low altitude spacecraft DEMETER in which MLR event was found is shown in Figure 1.

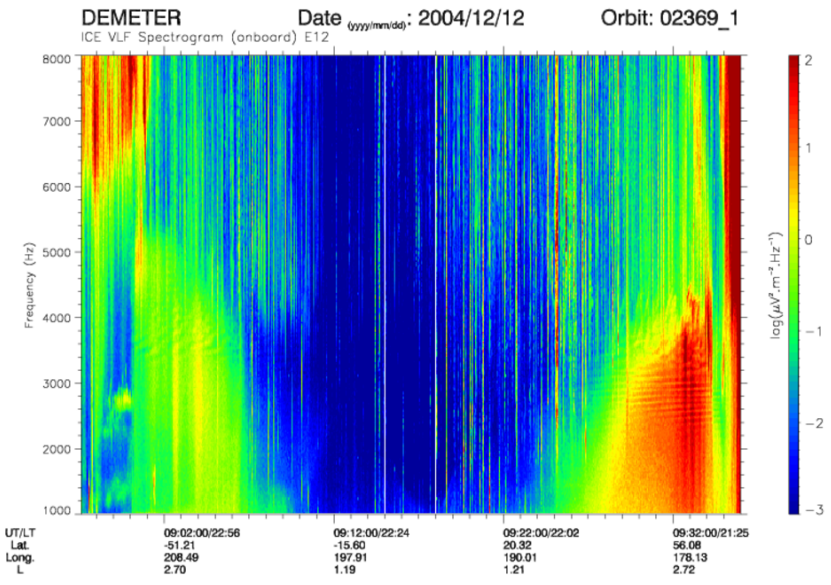

Figure 1: An example of MLR events detected by the DEMETER spacecraft on 12 December 2004 between 09:00 and 09:10 UT in the frequency range of about 3.2–4 kHz and between 09:27 and 09:34:30 UT in the frequency range of about 2.2–3.4 kHz.

In addition, so-called power line harmonic radiation (PLHR) exhibits a similar structure as MLR events. PLHR events are regarded as a man-made phenomenon. With regard to apparent similarities of MLR and PLHR structure, possible effects of human activity on MLR formation were also studied [Bullough, 1995]. Nevertheless, Rodger *et al.* [1999] and Rodger *et al.* [2000a] studied MLR events observed at Halley in Antarctica and Rodger *et al.* [2000a] finally concluded that MLR is most likely of a natural origin. This statement has been currently commonly accepted. Ground-based MLR observations typically last about 30 minutes and they preferably occur after periods of enhanced geomagnetic activity [Rodger *et al.*, 2000b].

A systematic study of spacecraft MLR measurements was first performed by Rodger *et al.* [1995]. An analysis of MLR events measured by International Satellites for Ionospheric Studies (ISIS) 1 and 2 revealed the existence of two different MLR types with different frequency drifts, frequency spacings and widths of individual spectral lines.

During recent years, MLR events were frequently analyzed using measurements performed by the low-altitude spacecraft DEMETER (see below) [e.g., Parrot *et al.*, 2005, 2007; Němec *et al.*, 2007, 2009]. The results showed that the events were measured rather during the day than during the night and supported the prior results based on the ground-based measurements that they predominantly occur during or after the periods of enhanced geomagnetic activity [Němec *et al.*, 2009]. An analysis of a complete set of MLR events observed during the entire DEMETER mission (consisting of 1230 MLR events) was performed by Bezděková *et al.* [2015]. The study reveals a seasonal dependence of the number of observed events, peaking between November and April, and a statistical dependence of the MLR occurrence on specific variations of solar wind parameters.

Quasiperiodic Emissions

While MLR events are characteristic by the frequency modulation of the intensity, events characterized by the time modulation of the wave intensity are called quasiperiodic (QP) emissions. These events are usually observed in the frequency range between about 0.5 and 4 kHz. The time separations between consecutive QP elements called modulation periods are a characteristic feature of an individual QP event, which can vary from some tens of seconds up to a several minutes [Helliwell, 1965]. An example of a QP emission measured by the DEMETER spacecraft is shown in a frequency-time spectrogram in Figure 2.

Similarly to MLR, first observations of QP emissions were performed by ground-based stations [Carson *et al.*, 1965; Helliwell, 1965]. Based on the first ground measurements, a classification of QP emissions was suggested [Kitamura *et al.*, 1969; Sato *et al.*, 1974]. QP emissions of "type 1" were detected simultaneously with geomagnetic ULF pulsations of a comparable period. However, periods of the ULF pulsations were sometimes different than the QP modulation periods or the pulsations were even completely absent during a detection of QP. In these cases, QP emissions were classified as QP of "type 2".

It is commonly believed that QP emissions originate in the equatorial plane preferably at large radial distances close to the plasmapause [Sato and Kokubun,

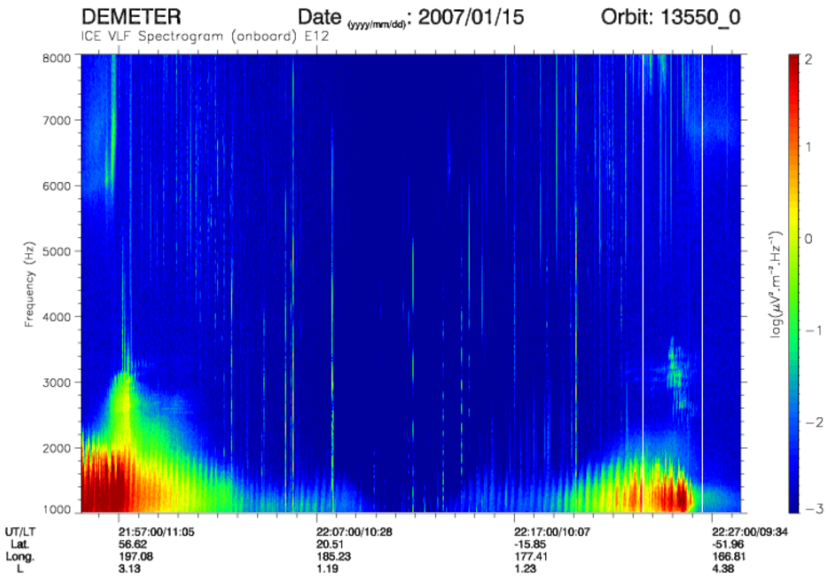

Figure 2: An example of QP events detected by the DEMETER spacecraft on 15 January 2007 between 21:55 and 22:09 UT in the frequency range of about 1–2.2 kHz and between 22:14 and 22:26 UT in the frequency range of about 1–1.8 kHz.

1980; Morrison, 1990]. Regarding their origin, two possible generation mechanisms have been proposed.

The first mechanism is based on the idea that a compressional ULF wave periodically modulates a source region and resonance conditions therein, resulting in the formation of QP emissions [Chen, 1974; Sato and Fukunishi, 1981]. An alternative mechanism suggested by Bespalov and Trakhtengerts [1976] is based on the idea that QP emissions are formed by an auto-regulating cyclotron instability in a region with enhanced cold plasma density. According to the model, essential free energy needed for the wave generation is provided by energetic electrons with an anisotropic distribution function, possibly coming to the source region via magnetic drift. In some sense, these two respective approaches correspond to QP emissions of type 1 and type 2 defined above. However, the type 1 and type 2 QP classification was developed using ground-based measurements and Sazhin and Hayakawa [1994]; Tixier and Cornilleau-Wehrlin [1986] showed that it is not suitable to be directly used also for spacecraft measurements.

An analysis of conjugate QP observations performed by several instruments at different locations can help to reveal the propagation properties of the events and their spatiotemporal variability. Previous analyses of such type, [e.g., Titova *et al.*, 2015] reported that a QP event usually exhibits the same frequency-time structure and modulation period over a large spatial region.

Although a formal QP structure is maintained, observations of individual QP elements measured at different radial distances at comparable azimuths can be detected with certain time delays, reaching the order of a few seconds, [Martinez-Calderon *et al.*, 2016]. The time delays between observations of QP elements at locations signif-

icantly separated in azimuth ($\sim$ tens of degrees) can be more than tens of seconds. QP propagation is not slow enough to be responsible for such long time delays. Němec *et al.* [2016] suggested instead that the propagation of a ULF compressional wave responsible for the formation of a QP emission is slow enough to lead to such high time delays.

Last, but not least, previous results based on both ground-based and low-altitude spacecraft measurements indicated that QP emissions are primarily observed on the dayside [Morrison *et al.*, 1994]. However, QP measurements at larger radial distances did not confirm any significant local time preference of the event occurrence [Němec *et al.*, 2018]. A detailed comparison of QP measurements of the low-altitude spacecraft DEMETER (altitude of about 700 km) and the pair of Van Allen Probes spacecraft operating on highly elliptical orbits almost in the equatorial plane (apogee altitude of about 32,000 km) was performed by Němec *et al.* [2020].

Data Sets

The main aim of the thesis is to analyze conjugate observations of QP emissions by a ground-based station and spacecraft. Hence, a description of two spacecraft missions (DEMETER and Van Allen Probes) and a ground-based station (Kannuslehto in northern Finland) follows. Additionally, due to the included study of solar wind effects on the wave properties, source of data related to solar wind parameters (OMNI data) is introduced.

DEMETER Spacecraft

DEMETER (an acronym for *Detection of Electro-Magnetic Emissions Transmitted from Earthquake Regions*) spacecraft was a French low-altitude satellite operating between July 2004 and December 2010. The original altitude reached about 710 km, but since December 2005 it was decreased to about 660 km. The satellite was operating on an almost Sun-synchronous circular orbit which led to basically only two possible magnetic local time (MLT) measurement intervals – either about 10:30 or 22:30 h. Within one day, the spacecraft performed 14 orbits.

Only the electric field measurements are used in the thesis. In the frequency range from 20 Hz to 20 kHz (VLF) these consist of onboard calculated power spectral densities in 1,024 linearly spaced frequency channels. The time resolution is about 2 s and the frequency resolution is about 19.53 Hz.

Van Allen Probes

Van Allen Probes (initially called *Radiation Belt Storm Probes*, RBSP) was a set of two satellites (RBSP A, RBSP B) launched in August 2012 and measuring till October 2019 which primarily focused on observing dynamics of the radiation belts.

RBSP operated on highly elliptical and nearly identical orbits in the equatorial plane with inclination about 20°. Radial distances reached between about 1.1 R_E and 5.8 R_E, which allowed the spacecraft to detect a broad area of the radiation

belts, covering a full range of magnetic local time (MLT) and geomagnetic longitude combinations.

Data used in the present thesis were in the frequency range between 10 Hz and 12 kHz divided into 64 quasi-logarithmically distributed channels. The time resolution of the data is 6 s. From the available multicomponent data wave propagation parameters, such as planarity, ellipticity, wave and Poynting vector directions, were calculated via singular value decomposition method as developed by Santolík *et al.* [2003] and other techniques introduced by Santolík *et al.* [2001, 2010].

The onboard wave measurements further allowed to evaluate the local plasma number density [Kurth *et al.*, 2015]. Moreover, the position of plasmapause (L_{pp}) was also estimated as the innermost position where the plasma number density falls below 100 cm^{-3}.

Kannuslehto Station

Among others, ground-based VLF measurements were performed by the Kannuslehto station located in northern Finland. The location of the station in geographic coordinates is 67.74° N; 26.27° E, which corresponds to L-shell of about 5.5. The station is managed by Sodankylä Geophysical Observatory (SGO), Sodankylä, Finland.

The measurement is realized by two orthogonal vertical magnetic loop antennas oriented in the north-south and east-west directions. Both loops cover 10x10 m and have 10 turns, and they thus reach the effective area of 1000 m^2. The antennas work in the frequency range 0.2–39 kHz with a sampling frequency 78,125 Hz. The receivers exhibit an extraordinary sensitivity ($\approx$ 0.1 fT) and a wide dynamic range (up to 120 dB). The station operates during campaigns, which are typically performed during the winter season and usually last several months.

To get power spectral densities of magnetic field fluctuations as measured by the Kannuslehto station, fast Fourier transform is performed. To compare the measurements with other instruments measuring only power spectral densities of electric field fluctuations (e.g., DEMETER), magnetic field fluctuations measured by Kannuslehto are recalculated to corresponding electric field fluctuations. Assuming the refractive index on the ground equals 1, electric field power spectral densities can be obtained by multiplying the Kannuslehto measured magnetic field fluctuations by the factor c^2, where c denotes the speed of light.

OMNI Data

OMNI data set covers a collection of solar wind interplanetary magnetic field and plasma parameters measured by several spacecraft operating either in geocentric orbits or near Lagrange L1 point. Thus, the obtained data represent values defining the solar wind near the Earth. Satellites like Wind, ACE, or ISEE 3 are used. The time of data is recalculated from the position of their detection to the position of the bow shock nose. Parameters used in the present thesis are the interplanetary magnetic field (IMF) magnitude, proton density, flow speed, and flow pressure. The used time resolution is 1 hour.

Aims of the Thesis

Although plasma-wave interactions represent a crucial aspect for most of the processes observed in the Earth's magnetosphere, regarding them, there are still open problems with no satisfactory answers. One of the most burning issues, solution of which could allow to better understand also other magnetospheric phenomena, is the missing understanding of generation mechanisms of certain wave phenomena observed in the Earth's magnetosphere. Every single detail describing their behavior in the system could once become relevant for understanding how they originate and propagate. From this point of view, it is important to statistically investigate the observed wave phenomena and search for general features about how, when, and where they are formed and how they propagate.

The present thesis is mainly focused on an analysis of multipoint observations of quasiperiodic emissions. The origin of these wave phenomena observed in the inner magnetosphere since 60's [Carson *et al.*, 1965; Helliwell, 1965] is not fully understood, although two main scenarios have been suggested (see above). Generally, the events can be observed by particular instruments, both space and ground. However, single point observations do not allow to distinguish between spatial and temporal variations. The main advantage of multipoint observations is hence a possibility to distinguish these two types of variations and possibly trace the wave propagation. In the ideal case, both spacecraft and ground-based station measurements are available and it is easy to identify the spatial variations as ground signal represents a convenient measure of temporal variations usable for a normalization of the satellite data. Alternatively, simultaneous measurements of several spacecraft can be used.

In the first approach, a case study of multipoint observations of QP emissions (a spacecraft, a ground-based station) is presented in the thesis. This represents a typical stance to such analysis. A single event can be usually easily detected by several instruments and, eventually, a ray tracing can be performed [e.g., Martinez-Calderon *et al.*, 2016]. However, this cannot capture the overall features of the wave propagation and it cannot be used to infer general wave behavior. This is why also a statistical analysis of conjugate observations is needed. Results of a statistical study of multipoint QP observations (two spacecraft, a ground-based station) are presented further.

Not only the effect of a wave propagation at different locations, but also an impact of the solar wind on the wave phenomena is a crucial aspect for investigation of their nature. It is commonly known that the solar wind significantly affects the magnetospheric regions and present phenomena. Concrete effects of solar wind parameters on the quasiperiodic emission properties (such as maximal intensity and modulation period) were recently studied [Bezděková, 2017; Bezděková *et al.*, 2019]. However, quasiperiodic emissions do not represent the only wave events of unexplained origin. Effects of solar wind parameters on perhaps even more mysterious magnetospheric line radiation are investigated, too.

Finally, an alternative possibility how to investigate effects of interplanetary shocks on general wave activity in the Earth's magnetosphere is presented. For this purpose, a principal component analysis was used and compared with a more traditional method of moving averages.

Conjugate Observations of QP Events

As mentioned above, the main results of the present thesis are based on the statistical analysis of conjugate QP observations. In this case, the measurements of two spacecraft (Van Allen Probes) and a ground-based station (Kannuslehto) were analyzed. Altogether, 26 simultaneously detected events were investigated. Such statistics represents a unique approach to the problem, as conjugate events were up to date typically studied in terms of case studies.

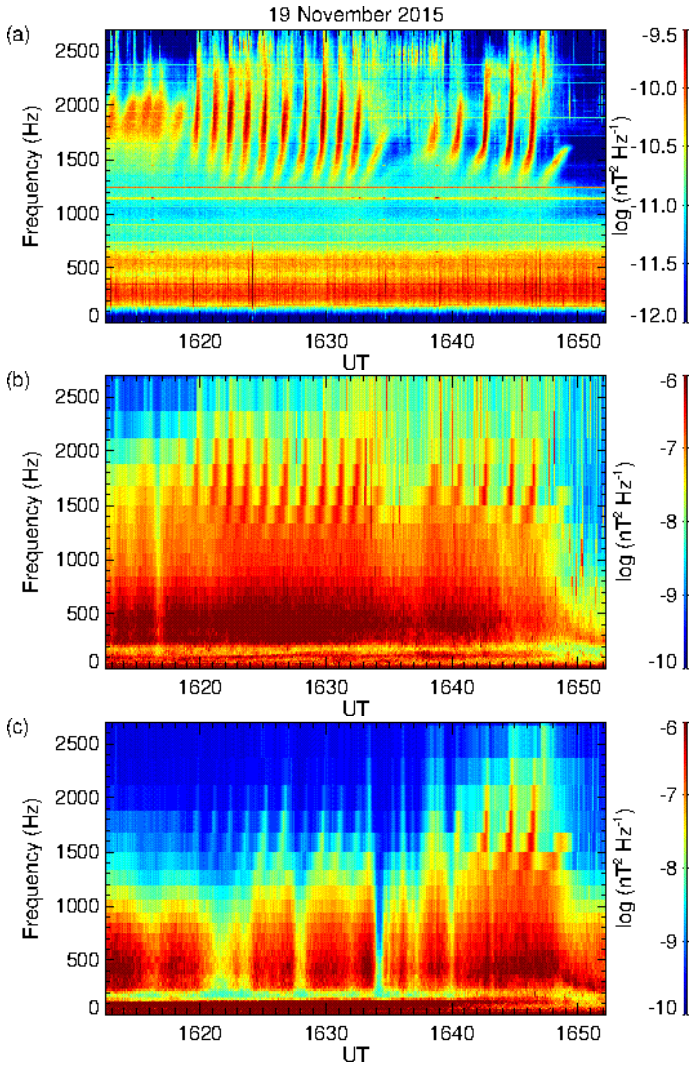

Figure 3: Frequency-time spectrograms measured by (a) the Kannuslehto station, (b) RBSP A, and (c) RBSP B during the conjugate observations of a QP event on 19 November 2015 between 16:18 and 16:50 UT. The QP event was measured in a frequency range between about 1200 and 2400 Hz. Although the event was actually observed by the Kannuslehto station over a much longer time interval, the depicted time interval corresponds to the period when the event was detected simultaneously by all the three instruments (adopted from Bezděková *et al.* [2020]).

The analysis was performed using measurements obtained between September 2012 and November 2017. While Van Allen Probes data continuously cover

the investigated time interval, the Kannuslehto station operated in nine distinct campaigns which include about 550 measurement days.

It happened only once that all the three available instruments (i.e., both Van Allen Probes spacecraft and the Kannuslehto station) simultaneously detected a single QP event. This event was observed on 19 November 2015 from 16:18 to 16:50 UT in the frequency range of about 1200–2400 Hz and it is shown in Figure 3. Despite the low time resolution of the spacecraft data, it is apparent that the temporal intensity variations correspond to each other in all three panels. Moreover, the observed frequency-time structure of individual QP elements is the same.

Notice an obvious gap between the consecutive QP elements around 16:36 UT and the increase of the time separations between consecutive QP elements after the gap. This unexpected event property is discussed in the thesis. Note that the time interval plotted in Figure 3 corresponds to the conjugate measurement time of the event, while the Kannuslehto station observed the QP emissions also before this period.

To better visualize the positions of the spacecraft during the simultaneous QP measurements, Figure 4 was created. It shows field-aligned projections of the RBSP A and RBSP B orbits during the observations of conjugate QP events. The map is drawn in geomagnetic coordinates. The thick red and blue curves, corresponding to RBSP A and RBSP B, respectively, show projections of orbits during the conjugate observations. The thin curves denote the projections of RBSP at the times when only one instrument (typically the Kannuslehto station) observed the events. Due to the relatively long duration of some events (several hours), the drawn projections are limited to within 30 minutes from the time intervals of conjugate observations as the projections showing the entire event duration would make the plot quite messy. The field-aligned projections were calculated using the International Geomagnetic Reference Field model (IGRF, Thébault *et al.* [2015]) and the T89 magnetic field [Tsyganenko, 1989] model. The position of the Kannuslehto station is depicted by the black cross at 119.8° geomagnetic longitude and 64.4° geomagnetic latitude.

It can be seen that the events were typically observed within 40° of geomagnetic longitude from the Kannuslehto location. Moreover, along with Kannuslehto, RBSP A mostly detected the QP emissions. However, some rather isolated events were observed simultaneously in spite of the longitudinal separation of the instruments reaching more than 100°.

Besides the conjugate observations of QP events by instruments close to each other, there are simultaneous QP measurements at the times when their azimuthal separation is considerable. This suggests that QP emissions can at times occur over a wide range of geomagnetic longitudes. However, it is difficult to explain such an azimuthal spread by the unducted propagation, which usually tends to remain close to a given magnetic meridian [see e.g., Hayakawa, 1987, and references therein]. Thus, in some cases, a large longitudinal extent of the QP source seems to be necessary.

The spatial separation between RBSP and Kannuslehto in terms of the distribution of MLT and L-shell differences during the conjugate QP observations is analyzed in Figure 5. The distribution of distances between RBSP and Kannuslehto

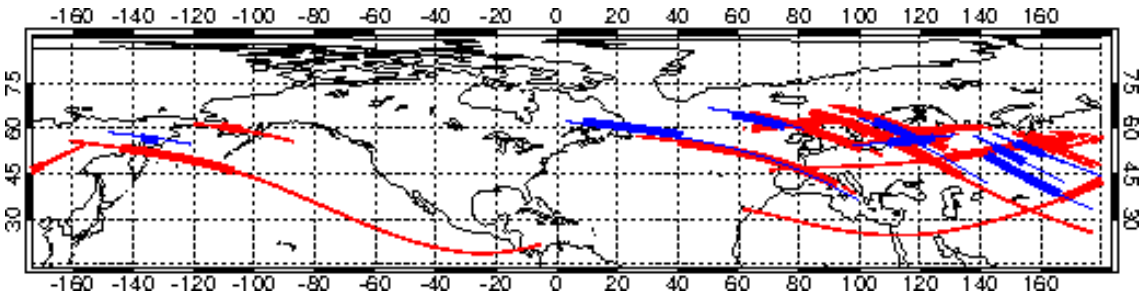

Figure 4: Field-aligned projections of the RBSP A (red curves) and RBSP B (blue curves) spacecraft orbits on the ground during the times of conjugate QP observations in geomagnetic coordinates. The thin curves denote the intervals when at least one instrument (either one of the spacecraft or the ground station) detected the event, while the simultaneous observations of QP emissions by the spacecraft and the Kannuslehto station are depicted by the thick curves. The location of the Kannuslehto station is drawn by the black cross (adopted from Bezděková *et al.* [2020]).

positions for all Kannuslehto measurement times during the entire nine campaigns covering the analyzed time interval (September 2012 – November 2017) is shown in Figure 5a. The distribution of spatial separations at the times of the conjugate QP event measurements is depicted in Figure 5b. The longest integral time of conjugate observations occurred at $L_{RBSP} - L_{KAN}$ between -3 and -1, while in the $|\Delta$ MLT$|$ domain it basically holds that the longest integral times of conjugate observations occur preferably during the lowest separations. Figure 5c shows the occurrence rate of simultaneously detected QP emissions (i.e., the ratio of simultaneous and total measurement durations) dependence on the spatial separation of the instruments. It still holds that the dependence on the L-shell difference is substantial, while the simultaneous observations occur preferentially during small $|\Delta$ MLT$|$.

Note that the negative $L_{RBSP} - L_{KAN}$ differences correspond to the situations when the Kannuslehto L-shell is larger than the RBSP L-shell. Since this is a preferable situation for the conjugate QP measurements, one can deduce that QP emissions detected by RBSP are generally located inside the plasmasphere (as shown by Němec *et al.* [2018]), while comparatively large L_{KAN} (≈ 5.5) is usually well outside the plasmasphere [e.g., Kwon *et al.*, 2015]. Indeed, most of the analyzed events were observed inside the plasmasphere (not shown). The wave arrival directions measured at Kannuslehto (not shown) were typically oriented to the station from the south or north (there is a $\pm 180°$ ambiguity when detecting the direction). Such orientation corresponds to the assumption of the event generation in the equatorial plane and the consecutive wave propagation within the plasmasphere [Němec *et al.*, 2018], possibly ducted by the plasmapause when propagating to low altitudes [Hayosh *et al.*, 2016].

The obtained L-shell separations provide a rough estimate of the QP radial extent. Unducted wave propagation can possibly explain the observed radial differences of about 2 R_E [Němec *et al.*, 2014; Martinez-Calderon *et al.*, 2016]. Remark that in such case, the time delays between the detection of QP elements at different

locations should be observed as the wave propagates from the source region. Unfortunately, the relatively low time resolution of the used RBSP data (6 s) does not allow to perform this analysis, as it is comparable to or sometimes even larger than the expected time delays.

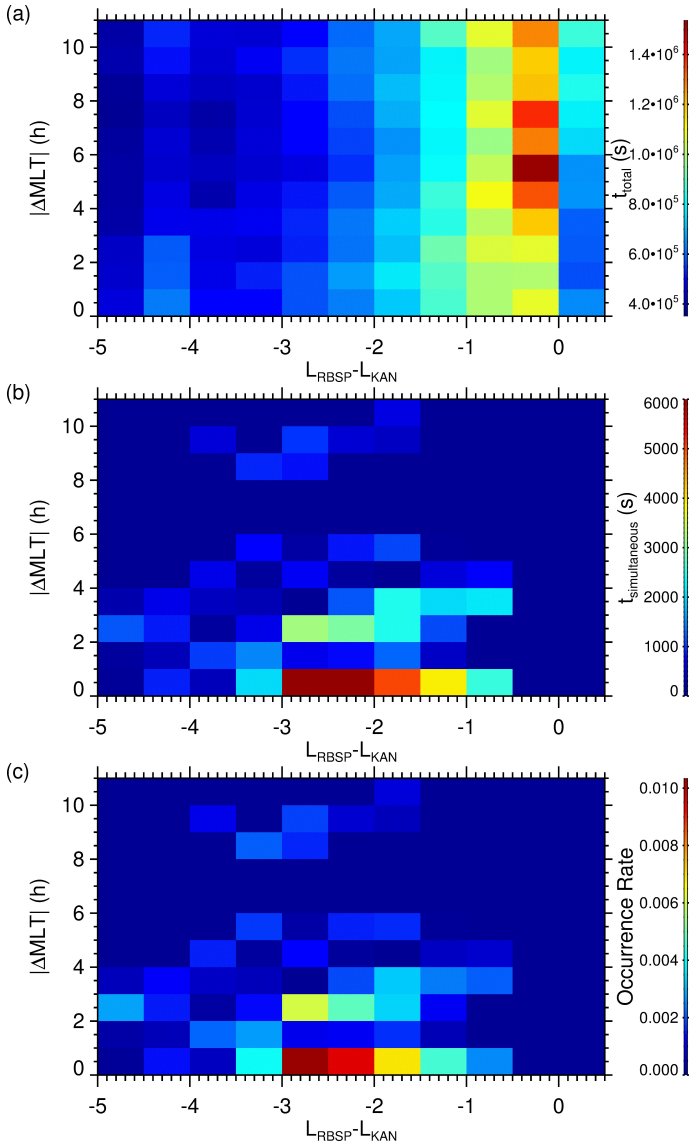

Figure 5: L-shell and MLT distances between the RBSP spacecraft and the Kannuslehto station. (a) Total durations of the measurements during the Kannuslehto campaigns in given ΔL–$|\Delta MLT|$ bins. (b) Same as (a), but for the total durations of simultaneously detected QP emissions. (c) Occurrence rate of the conjugate measurements of QP emissions as a function of the L-shell distance (x-axis) and MLT distance (y-axis) (adopted from Bezděková *et al.* [2020]).

Connection between MLR and QP

According to the definition given above, both MLR and QP events are characterized by a nearly periodic modulation of the wave intensity. While in the case of MLR the intensity modulation occurs in the frequency domain, the QP intensity modulation is observed in the time domain. Alternatively, the number of individual event elements spanning over a given frequency or time interval is opposite for each type of the events.

In most cases, the distinction between MLR and QP events is quite clear. However, in few cases the classification of the type of the event starts to be tricky and it is rather ambiguous. In Figure 6, an example of such event is depicted. The event was detected by the DEMETER spacecraft on 16 April 2005 between about 11:13 and 11:17 UT in the frequency range 1.8–3.5 kHz. In the frequency-time spectrogram in Figure 6a, the event is marked by the black rectangle. Figure 6b shows a detailed view of the event. The frequency drift of the event substantially fluctuates; while being comparatively low at low frequencies, it gradually increases toward higher frequencies. Hence, although the event part at lower frequencies is more or less MLR-like, the part at higher frequencies should be rather classified as QP.

Moreover, statistical results concerning QP events [Hayosh *et al.*, 2014] and MLR events [Bezděková *et al.*, 2015] based on the DEMETER data set suggest a possibility that the two types of events are related. Both the MLR and QP events occur preferentially after increased geomagnetic activity periods, during daytime rather than during nighttime, and their occurrence rate is lowest at geomagnetic longitudes corresponding to the SAA. Actually, while MLR events might be considered as the frequency modulation of hiss emissions, the QP emissions could be regarded as the time modulation of hiss emissions. However, this idea is rather questionable and a possible relationship of all three phenomena needs to be further investigated.

Following the ideas mentioned above, it seems to be useful to study both the MLR and QP properties of the events observed at the same or at least at similar times and to search for their possible connection. MLR and QP events observed within one DEMETER orbit from each other, i.e., within less than about two hours, and in the same MLT sector were thus considered. Properties of such events were assumed to be potentially related. Altogether, 260 MLR-QP event pairs fulfilled this condition and their properties were compared. The results are shown in Figure 7. Remark that the occurrence of the found event pairs seems to be purely random and no specific geomagnetic or any other conditions preferable for their occurrence were identified.

The relation of the QP modulation periods and the MLR frequency spacings is depicted in Figure 7a. Each point in the plot corresponds to a detected MLR-QP pair. The black horizontal lines show median values in given MLR frequency spacing bins. The red line separates the plot into the regions with QP events with short (< 20 s) and long (> 20 s) modulation periods. The analysis was performed separately for these two groups of QP emissions, as it appears they may eventually behave rather differently [Bezděková, 2017; Bezděková *et al.*, 2019]. No clear relation between the parameters can be seen. Figure 7b shows the dependence of the maximal QP intensity on the MLR frequency spacing. The red points correspond to the MLR-

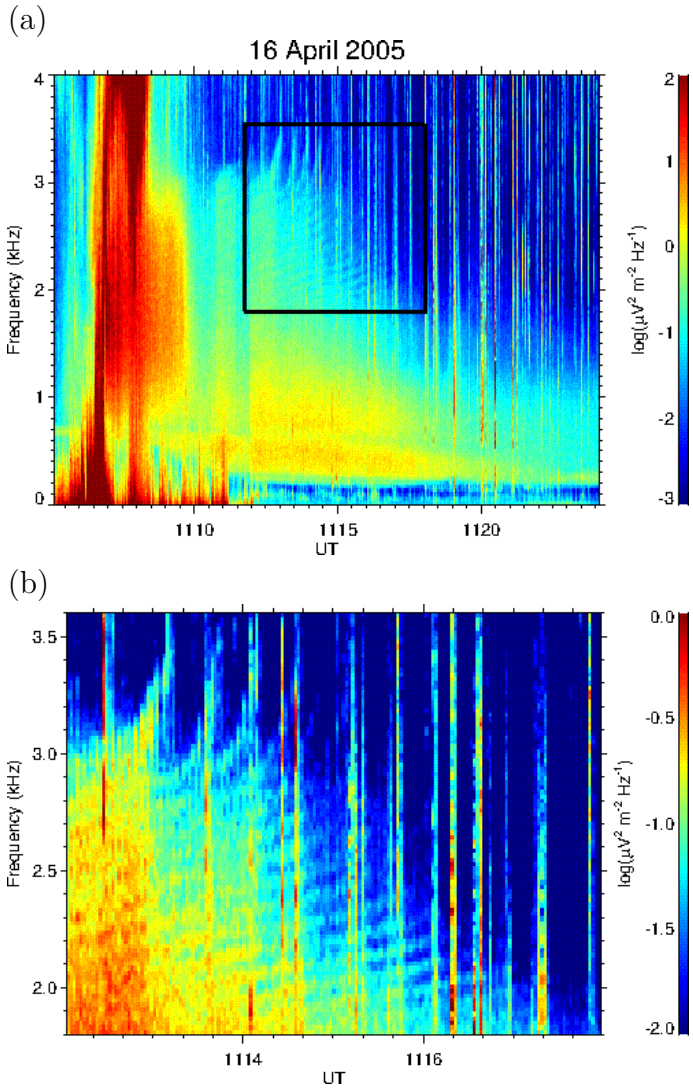

Figure 6: (a) Example of frequency-time spectrogram of an event whose classification as MLR or QP is rather ambiguous. The event occurred on 16 April 2005 between 11:13 and 11:17 UT at frequencies between about 1.8 and 3.5 kHz. The frequency-time interval of the event is bounded by the black rectangle. At low frequencies, the observed frequency drift is rather low and the event can thus be classified as MLR. However, the frequency drift gradually increases with the frequency and at higher frequencies, the event might be rather considered as QP-like. (b) Zoomed frequency-time spectrogram containing the discussed event. Note that in this part of the frequency-time spectrogram the color scale used in (a) tends to be monotonous and the color scale in (b) was hence changed in order to better highlight the elements of the event (adopted from Bezděková *et al.* [2019]).

QP pairs with QP modulation periods above 20 s, while the blue points show the results obtained for the pairs including QP events with modulation periods below 20 s. The red and blue lines depict the corresponding median values. Again, no clear relation between the QP intensities and the corresponding MLR frequency spacings

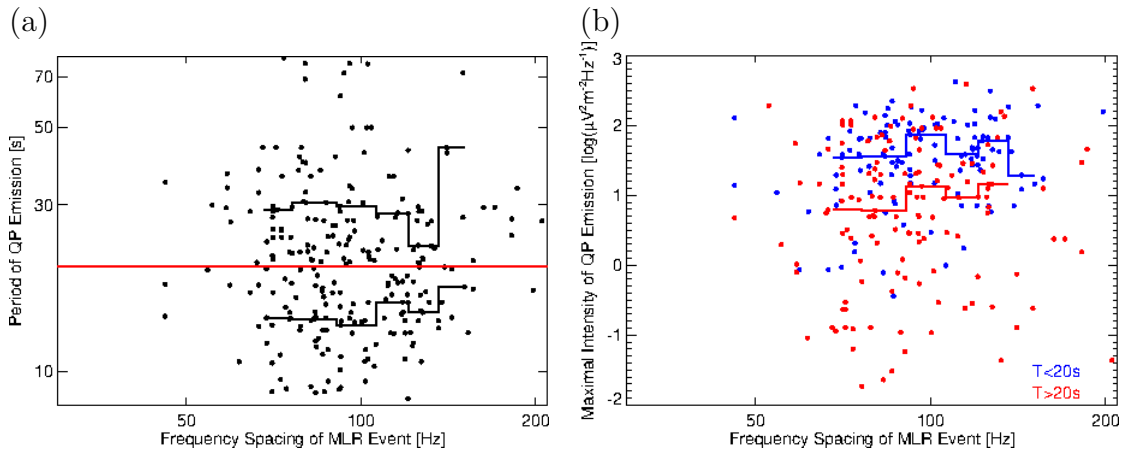

Figure 7: (a) Dependence of the QP modulation periods on the MLR frequency spacings for the events observed at the same times. The threshold modulation period of 20 s is denoted by the red horizontal line. The median modulation periods drawn by the black lines were determined separately for events with modulation periods shorter and longer than given threshold. (b) Dependence of the maximal QP intensities on the MLR frequency spacings for the simultaneously observed events. The data points corresponding to the individual MLR-QP pairs and appropriate median values obtained for QP events with modulation periods longer than 20 s are drawn by the red color. The results obtained for QP emissions with modulation periods shorter than 20 s are shown in blue (adopted from Bezděková *et al.* [2019]).

was found.

Based on the obtained results, there seems to be no apparent relation between simultaneously observed MLR and QP events. Additionally, while the QP nighttime occurrence rate is extremely low [Hayosh *et al.*, 2014], MLR events are observed quite regularly also during the night [Bezděková *et al.*, 2015]. Although the analyzed MLR and QP events were observed very close to each other (in the time domain), their simultaneous occurrence thus appears to be only a lucky coincidence with no straightforward physical explanation.

Influence of Interplanetary Shocks on the Overall VLF Wave Activity

The effect of interplanetary shocks on the wave intensity in the VLF range detected by a low-altitude spacecraft (DEMETER) is studied in this section. The analysis was performed by two different methods – averaging over given time intervals and principal component analysis (PCA) – and then compared.

Daytime measurements performed during the entire DEMETER mission are used in this section. Altogether, 29,335 daytime frequency-time spectrograms obtained during the 6.5 years of the spacecraft mission were analyzed. Note that in total the satellite performed 57,574 half orbits.

The effect of interplanetary (IP) shocks on wave intensities measured by the

DEMETER spacecraft was investigated separately for each shock type – fast forward (FF), fast reverse (FR), slow forward (SF), and slow reverse (SR) shocks. IP shocks observed within the DEMETER mission by the Wind spacecraft (located close to the L1 point) were found by an automatic procedure and manually verified [Kruparova *et al.*, 2013]. Altogether, 225 IP shocks were detected. Out of them, 87 were classified as FF, 31 as FR, 59 as SF, and 48 as SR shocks.

The average evolution of the overall wave intensity measured by the DEMETER spacecraft around the times of the shock arrivals is shown in Figure 8. The variations of the wave intensity measured from 5 hours before to 24 hours after the shock arrival are depicted. The plotted wave intensities were calculated as moving averages over 30 minute long intervals considering only measurements in the geomagnetic latitudinal range $40° - 60°$. This range corresponds to geomagnetic latitudes where the wave phenomena studied in the present thesis typically occur. The times of the shock arrivals are drawn by the dashed white lines.

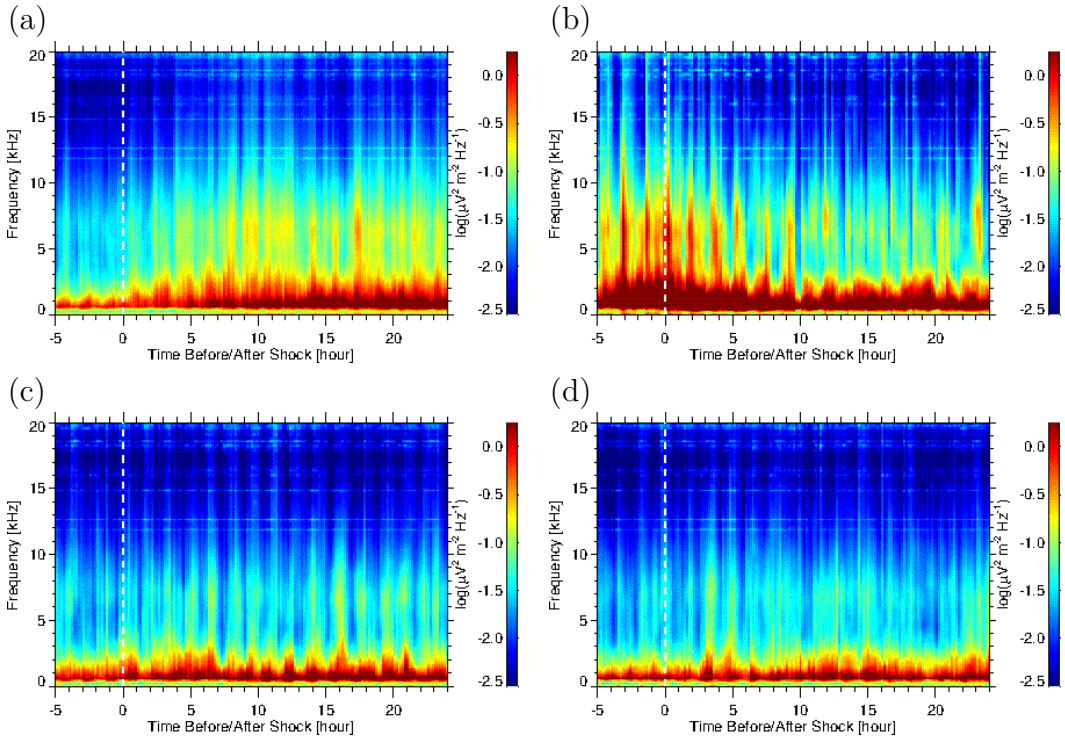

Figure 8: Average wave intensity detected by the DEMETER spacecraft around the (a) FF, (b) FR, (c) SF, and (d) SR shock arrivals, respectively. Intensity fluctuations in the time interval from 5 hours before to 24 hours after the shock arrival are shown. Only data obtained at geomagnetic latitudes between 40° and 60° are included in the analysis. Moving averages over a 30 minute long time window were used to smooth the plots (adopted from Bezděková *et al.* [2018]).

It can be seen that the wave intensity considerably varies (usually increases) around the times of the shock arrivals. The increase of the wave intensity occurs preferentially at frequencies lower than about 10 kHz. Note that in the case of FR shocks, the wave intensity increase is also apparent at higher frequencies. Out

of all obtained variations, the wave intensity increases most before the FR shock arrival in the frequency range up to around 3 kHz (Figure 8b). The wave intensity is predominantly increased before the FR shock arrival and after the shock, it starts to decrease slowly.

The effect of the FR shock arrival on the wave intensity is quite intricate. Only 31 FR shocks were found in the Wind spacecraft data during the DEMETER mission, which is the lowest number out of all analyzed shock types. However, the effect of the shock presence on the wave intensity is evident. The maximum wave intensity increase observed before the FR shock arrival can be explained by the coupling between FF and FR shocks [Smith and Wolfe, 1976], since the shocks usually form a pair where a FF shock is followed by a FR shock. Notice that the wave intensity is significantly increased up to about 10 hours after the FR shock arrival, which indicates that favorable conditions for the wave intensity enhancement persist for several hours after the shock.

Also in the case of FF shocks, a substantial increase of the wave intensity occurs (Figure 8a). However, the situation is reverse. While there is basically no intensity increase before the FF shock arrival, the intensity increases considerably immediately after the FF shock arrival. The maximal wave intensity occurs around 10 hours after the FF shock arrival, and it stays increased more or less for the remaining part of the analyzed time interval. In fact, the time of the maximum wave intensity approximately corresponds to the time of the peak Kp index value (not shown). The results are also in agreement with the maximum value of the first principal component coefficients discussed further (see Figure 9a).

As Figures 8c,d show, for the slow shocks there is basically no apparent change of the wave intensity before or after the shock arrival. Thus, the slow shocks seem to be too weak to somehow significantly affect the wave intensity.

Remark the discrete character of the average intensities in Figure 8. This is likely due to the variety of half orbits at various times and locations where the wave intensity data contributing to individual time bins were measured and they thus could be significantly different. Furthermore, an unequal number of DEMETER data points were included in individual time intervals.

The analysis of the connection between the wave intensity and interplanetary shocks was further performed using the principal component analysis (PCA, e.g., Richardson [2009]).

Principal component analysis performs a transformation which effectively reduces the dimensionality of a given data set. It is frequently used for large sets of variables, as it transforms them into smaller ones, containing most of the information from the original sets. The reduction of the number of variables always implies losts of information, but the highly-valued advantage of PCA is its simplicity. The trick consists in how to reduce the number of data set variables and at the same time, maintain as much information as possible. This is achieved by the fact that the first few principal components carry most of the information.

For the present purpose frequency-time spectrograms measured by the DEMETER spacecraft are considered as the PCA *variables*. However, considering that on the time scales of a single half orbit most of the observed intensity variations are spatial, i.e., due to the spacecraft movement, the time dependence was recalculated

to geomagnetic latitude dependence and the analysis was in fact performed using frequency-latitude spectrograms. Moreover, each spectrogram exhibits a latitudinal symmetry, as the spacecraft regularly crossed the equator. Consequently, two spectrograms were obtained from each of the 29,335 dayside half orbits. Altogether, 58,670 frequency-latitude spectrograms with the frequency resolution 156.25 Hz and latitudinal resolution 2° spanning the frequency range 0–20 kHz and latitudinal range $0° - 60°$ were used as the initial (large) data set. After the PCA calculation, a new set of variables – principal components – was obtained. Altogether, 3,840 principal components (i.e., frequency-geomagnetic latitude spectrograms forming a new principal component basis) were calculated.

Since the majority of the information is contributed in the first few components, only a handful of them are needed to characterize the original data with a sufficient accuracy. In our case, this actually means that a given original DEMETER spectrogram can be characterized by a set of coefficients calculated from its decomposition into the principal components.

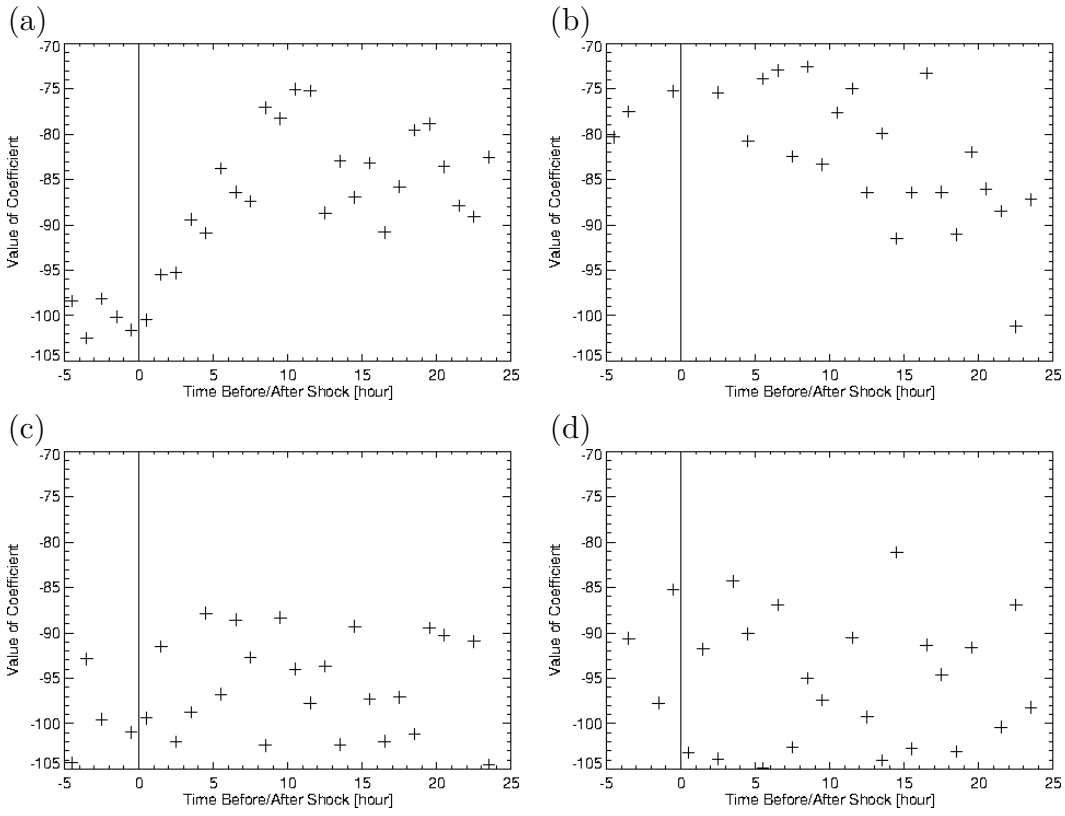

Figure 9: Mean values of the first principal component coefficients calculated with one hour time resolution as a function of the time relative to the (a) FF, (b) FR, (c) SF, and (d) SR shock arrival, respectively. The depicted time interval corresponds to the time interval used in Figure 8 (adopted from Bezděková *et al.* [2018]).

The idea of a characterization of each frequency-geomagnetic latitude spectrogram by only two coefficients corresponding to the first two principal components is used in Figures 9 and 10. The spectrograms measured during the same time interval

as depicted in Figure 8, i.e., from 5 hours before to 24 hours after the shock arrival, were all characterized by the linear coefficients corresponding to the first two principal components. The first two components carry most of the information and the other coefficients were thus not used further.

Figure 9 shows the variations of the mean values of the first principal component coefficients with respect to the time of the shock. The time of the shock arrival is depicted by the vertical black line. A strong dependence of the coefficient values on the time of the fast shock arrivals is apparent for both the FF and FR shocks. However, the observed trends are quite opposite. While before the FF shock arrival the coefficients are rather low and they gradually increase after the shock, the coefficients tend to decrease after the FR shock. In contrast, there is no clear dependence of the coefficients on the slow shock arrival times.

The evolution of the coefficients corresponding to the second principal component around the time of the shock arrival is depicted in Figure 10. The time of the shock arrival is again denoted by the vertical black line. Similarly to Figure 9, there is basically no dependence of the coefficients on the time of the slow shock arrival and an opposite trend is observed for the FF shocks and the FR shocks. While the coefficients increase after the time of the FF shock arrival, they tend to decrease after the FR shock arrival time.

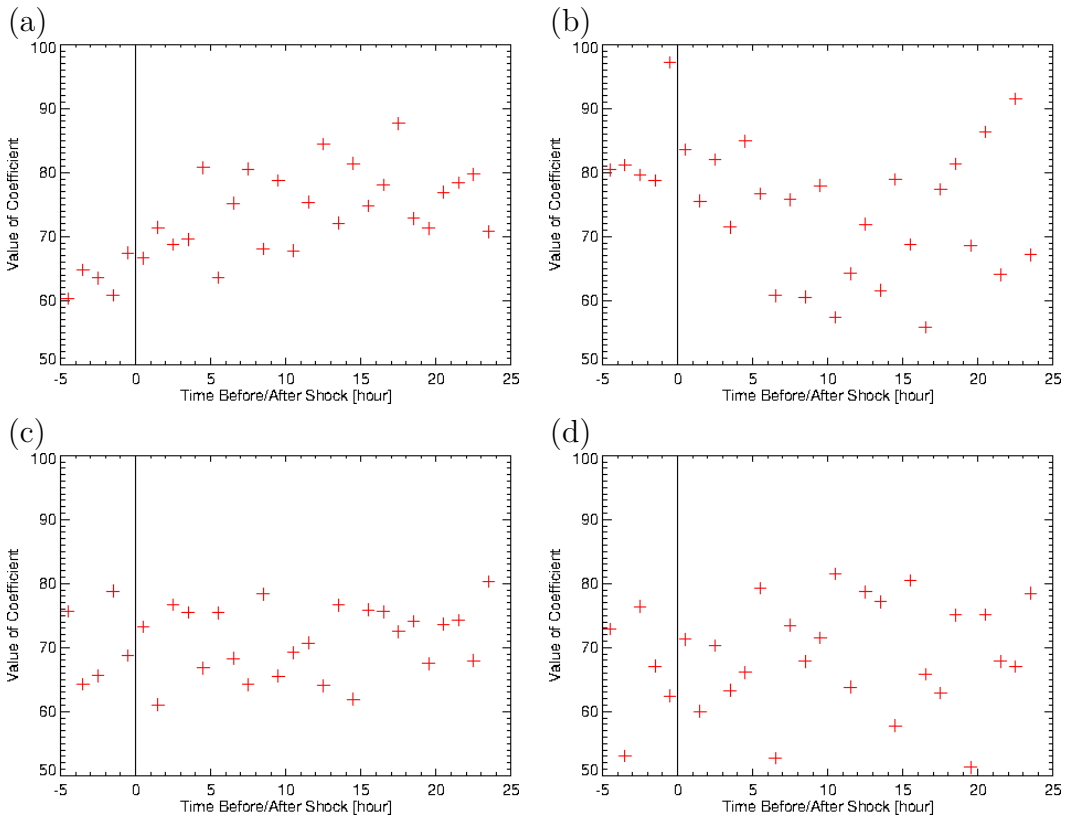

Figure 10: Same as in Figure 9, but for the second principal component coefficients (adopted from Bezděková *et al.* [2018]).

The results based on the PCA analysis shown in Figures 9 and 10 are in rough

agreement with the results obtained using moving averages depicted in Figure 8. However, their exact interpretation is more complicated, as the principal components do not correspond to measurable variables and they thus do not have a direct physical meaning. It seems feasible that in the case of the FF shocks, the first principal component (Figure 9a) is sufficient to describe the wave intensity fluctuations. This suggests that the variations of the wave intensity caused by the presence of a FF shock mainly correspond to wave characteristics described by the first principal component. Hence, the first principal component carries most of the information about the intensity variation affected by the FF shocks. In contrast, in the FR shock case, the times of the coefficient maximal values obtained for the first principal component (Figure 9b) do not correspond to the times of the maximal intensity as depicted in Figure 8b. Moreover, the decrease of the coefficient values is slower than it would correspond to the results shown in Figure 8b. All these observations indicate that also the information contained in the second principal component, as shown in Figure 10b, should be considered. Roughly speaking, the coefficients acquired for the second principal component seem to better correspond to the results depicted in Figure 8b. Considering the appropriate principal components, the importance of different principal component coefficients suggests that typical frequency-latitude intensity patterns are different for different shock types. However, the suggested interpretation of the PCA results is very rough and a deeper insight into the whole technique is necessary for a more thorough discussion. Above all, the physical interpretation of the principal components is a crucial task.

Conclusions

The thesis focused on whistler mode waves observed in the inner magnetosphere of the Earth in the VLF range (3 Hz–30 kHz), so-called quasiperiodic (QP) emissions and magnetospheric line radiation (MLR). Simultaneous observations of QP emissions, possible links between the MLR events and solar wind parameters, relationship between the studied wave phenomena, and the effect of interplanetary shocks on the overall VLF wave activity were studied.

The conjugate observations of QP emissions were analyzed using both the case and statistical approaches. The case study based on the simultaneous observations of a QP event on 26 February 2008 by the French low-altitude spacecraft DEMETER and the Finnish ground-based Kannuslehto station helped to develop a technique which was further used for a statistical analysis of conjugate QP observations. The statistical study of conjugate QP measurements performed by the two Van Allen Probes spacecraft and, again, by the ground-based Kannuslehto station focused mainly on the event spatial extent and intensity variations. Altogether, 26 simultaneously measured QP events were found between September 2012 and November 2017. The analysis of typical spatial separations during the conjugate event detections revealed that the instruments were usually separated less than 40° in geomagnetic longitude and between about 1 and 3 in L-shells. Moreover, event detections primarily at spacecraft L-shells lower than 5.5 confirm the results of previous studies suggesting that the events occur preferably inside the plasmasphere. A case study of a strange QP event with a gap in its structure and a subsequent increase of the modulation period was further performed. After excluding various scenarios of the gap origin, the event was finally interpreted as two closely related events.

Properties of MLR events, namely the frequency drift and frequency spacing, were compared to each other and the dependence of the MLR frequency spacings on the geomagnetic activity indices and solar wind parameters was analyzed. It was shown that larger MLR frequency drifts typically correspond to larger frequency spacings. Moreover, the MLR frequency spacings tend to increase during geomagnetically disturbed periods and at times of higher solar wind flow speeds.

A search for possible relationship between the MLR and QP event properties observed at the same times did not reveal any significant relation.

Dependence of the overall VLF wave intensities detected by the DEMETER spacecraft on the interplanetary shock arrivals was analyzed by two methods, i.e., using average intensities and the values of the first two principal component coefficients around the times of the shock arrivals. It was shown that the wave intensity variations depend significantly on the type of the shock. The effect of the slow shocks on the wave intensity is much lower than the effect of the fast shocks. Moreover, the evolutions of the overall geomagnetic activity in terms of Kp index around the times of the shock arrivals exhibit similar trends as observed for the wave intensities.

Although several new findings about the whistler wave modes were stated in the present thesis, there still remain plenty of unanswered problems which have to be addressed in the future.

References

T. F. Bell, J. P. Luette, and U. S. Inan. ISEE 1 observations of VLF line radiation in the Earth's magnetosphere. *J. Geophys. Res.*, 87(A5):3530–3536, 1982.

P. A. Bespalov and V. Yu. Trakhtengerts. Nonlinear oscillatory processes in the Earth's magnetosphere. *Radiophysics and Quantum Electronics*, 19(6):567–574, 1976.

B. Bezděková, F. Němec, M. Parrot, O. Santolík, and O. Kruparova. Magnetospheric line radiation: 6.5 years of observations by the DEMETER spacecraft. *J. Geophys. Res. Space Physics*, 120:9442–9456, 2015.

B. Bezděková, F. Němec, M. Parrot, O. Santolík, V. Krupař, and O. Kruparova. Influence of interplanetary shocks on ELF/VLF waves observed in the Earth's magnetosphere. In J. Šafránková and J. Pavlů, editors, *WDS'18 Proceedings of Contributed Papers âĂŤ Physics*, pages 85–92, Prague, 2018. Matfyzpress.

B. Bezděková, F. Němec, M. Parrot, M. Hajoš, J. Záhlava, and O. Santolík. Dependence of properties of magnetospheric line radiation and quasiperiodic emissions on solar wind parameters and geomagnetic activity. *J. Geophys. Res. Space Physics*, 124(4):2552–2568, 2019.

B. Bezděková, F. Němec, J. Manninen, G. B. Hospodarsky, O. Santolík, W. S. Kurth, and D. P. Hartley. Conjugate observations of quasiperiodic emissions by the Van Allen Probes spacecraft and ground-based station Kannuslehto. *J. Geophys. Res. Space Physics*, 125(6):e2020JA027793, 2020.

B. Bezděková. Vybrané vlnové jevy v zemské magnetosféře. Master's thesis, MFF UK, Praha, 2017.

K. Bullough. *Handbook of Atmospheric Electrodynamics*, volume 2, chapter Power Line Harmonic Radiation: Sources and Environmental Effects, pages 291–332. CRC Press, Boca Raton, 1995.

W. B. Carson, J. A. Koch, J. H. Pope, and R. M. Gallet. Long period very low frequency emission pulsations. *J. Geophys. Res.*, 70(17):4293–4303, 1965.

L. Chen. Theory of ULF modulation of VLF emissions. *Geophys. Res. Lett.*, 1(2):73–75, 1974.

M. Hayakawa. The generation mechanism of ELF hiss in detached plasma regions of the magnetosphere, as based on the direction finding results. *Mem. Natl. Inst. Polar Res., Spec. Issue*, 47:173–182, 1987.

M. Hayosh, F. Němec, O. Santolík, and M. Parrot. Statistical investigation of VLF quasiperiodic emissions measured by the DEMETER spacecraft. *J. Geophys. Res. Space Physics*, 119:8063–8072, 2014.

M. Hayosh, F. Němec, O. Santolík, and M. Parrot. Propagation properties of quasi-periodic VLF emissions observed by the DEMETER spacecraft. *J. Geophys. Res. Space Physics*, 43:1007–1014, 2016.

R. A. Helliwell, J. P. Katsufrakis, T. F. Bell, and R. Raghuram. VLF line radiation in the Earth's magnetosphere and its association with power system radiation. *J. Geophys. Res.*, 80:4249–4258, 1975.

R. A. Helliwell. *Whistlers and related ionospheric phenomena*. Stanford University Press, Stanford, California, 1965.

T. Kitamura, J. A. Jacobs, T. Watanabe, and R. B. Flint Jr. An investigation of quasi-periodic VLF emissions. *J. Geophys. Res.*, 74(24):5652–5664, 1969.

O. Kruparova, M. Maksimovic, J. Šafránková, Z. Němeček, O. Santolík, and V. Krupař. Automated interplanetary shock detection and its application to Wind observations. *J. Geophys. Res. Space Physics*, 118(8):4793–4803, 2013.

W. S. Kurth, S. De Pascuale, J. B. Faden, C. A. Kletzing, G. B. Hospodarsky, S. Thaller, and J. R. Wygant. Electron densities inferred from plasma wave spectra obtained by the waves instrument on Van Allen Probes. *J. Geophys. Res. Space Physics*, 120:904–914, 2015.

H.-J. Kwon, K.-H. Kim, G. Jee, J.-S. Park, H. Jin, and Y. Nishimura. Plasmapause location under quiet geomagnetic conditions (Kp $\leq$ 1): THEMIS observations. *Geophys. Res. Lett.*, 42(18):7303–7310, 2015.

C. Martinez-Calderon, K. Shiokawa, Y. Miyoshi, K. Keika, M. Ozaki, I. Schofield, M. Connors, C. A. Kletzing, M. Hanzelka, O. Santolík, and W. S. Kurth. ELF/VLF wave propagation at subauroral latitudes: Conjugate observation between the ground and Van Allen Probes A. *J. Geophys. Res. Space Physics*, 121(6):5384–5393, 2016.

K. Morrison, M. J. Engebretson, J. R. Beck, J. E. Johnson, R. L. Arnoldy, L. J. Cahill, D. L. Carpenter, and M. Gallani. A study of quasi-periodic ELF-VLF emissions at three Antarctic stations: Evidence for off-equatorial generation? *Ann. Geophys.*, 12:139–146, 1994.

K. Morrison. Quasi-periodic VLF emissions and concurrent magnetic pulsations seen at $L = 4$. *Planet. Space Sci.*, 38(12):1555–1565, 1990.

F. Němec, J. S. Pickett, and O. Santolík. Multispacecraft Cluster observations of quasiperiodic emissions close to the geomagnetic equator. *J. Geophys. Res. Space Physics*, 119:9101–9112, 2014.

F. Němec, G. B. Hospodarsky, B. Bezděková, A. G. Demekhov, D. L. Pasmanik, O. Santolík, W. S. Kurth, and D. P. Hartley. Quasiperiodic whistler mode emissions observed by the Van Allen Probes spacecraft. *J. Geophys. Res. Space Physics*, 123:8969–8982, 2018.

F. Němec, O. Santolík, M. Parrot, and J. J. Berthelier. Comparison of magnetospheric line radiation and power line harmonic radiation: A systematic survey using the DEMETER spacecraft. *J. Geophys. Res.*, 112, 2007.

F. Němec, M. Parrot, O. Santolík, C. J. Rodger, M. J. Rycroft, M. Hayosh, D. Shklyar, and A. Demekhov. Survey of magnetospheric line radiation events observed by the DEMETER spacecraft. *J. Geophys. Res.*, 114(A05203), 2009.

F. Němec, B. Bezděková, J. Manninen, M. Parrot, O. Santolík, M. Hayosh, and T. Turunen. Conjugate observations of a remarkable quasiperiodic event by the low-altitude DEMETER spacecraft and ground-based instruments. *J. Geophys. Res. Space Physics*, 121:8790–8803, 2016.

F. Němec, O. Santolík, G. B. Hospodarsky, M. Hajoš, A. G. Demekhov, W. S. Kurth, M. Parrot, and D. P. Hartley. Whistler mode quasiperiodic emissions: Contrasting Van Allen Probes and DEMETER occurrence rates. *J. Geophys. Res. Space Physics*, 125(4):e2020JA027918, 2020.

M. Parrot, F. Němec, O. Santolík, and J. J. Berthelier. ELF magnetospheric lines observed by DEMETER. *Ann. Geophys.*, 23:3301–3311, 2005.

M. Parrot, J. Manninen, O. Santolík, F. Němec, T. Turunen, T. Raita, and E. Macúšová. Simultaneous observation on board a satellite and on the ground of large-scale magnetospheric line radiation. *Geophys. Res. Lett.*, 34(L19102), 2007.

M. Richardson. Principal component analysis. `http://www.dsc.ufcg.edu.br/~hmg/disciplinas/posgraduacao/rn-copin-2014.3/material/SignalProcPCA.pdf`, 2009. online; last access: 19. 8. 2020.

C. J. Rodger, N. R. Thomson, and R. L. Dowden. VLF line radiation observed by satellite. *J. Geophys. Res.*, 100(A4):5681–5689, 1995.

C. J. Rodger, M. A. Clilverd, K. H. Yearby, and A. J. Smith. Magnetospheric line radiation observations at Halley, Antarctica. *J. Geophys. Res.*, 104(A8):17441–17447, 1999.

C. J. Rodger, M. A. Clilverd, K. Yearby, and A. J. Smith. Is magnetospheric line radiation man-made? *J. Geophys. Res.*, 105(A7):15981–15990, 2000.

C. J. Rodger, M. A. Clilverd, K. H. Yearby, and A. J. Smith. Temporal properties of magnetospheric line radiation. *J. Geophys. Res.*, 105(A1):329–336, 2000.

O. Santolík, F. Lefeuvre, M. Parrot, and J. L. Rauch. Complete wave-vector directions of electromagnetic emissions: Application to INTERBALL-2 measurements in the nightside auroral zone. *J. Geophys. Res. Space Physics*, 106(A7):13191–13201, 2001.

O. Santolík, M. Parrot, and F. Lefeuvre. Singular value decomposition methods for wave propagation analysis. *Radio Sci.*, 38(1):1010, 2003.

O. Santolík, J. S. Pickett, D. A. Gurnett, J. D. Menietti, B. T. Tsurutani, and O. Verkhoglyadova. Survey of Poynting flux of whistler mode chorus in the outer zone. *J. Geophys. Res.*, 115(A00F16), 2010.

N. Sato and H. Fukunishi. Interaction between ELF-VLF emissions and magnetic pulsations: Classification of quasiperiodic ELF-VLF emissions based on frequency-time spectra. *J. Geophys. Res.*, 86(A1):19–29, 1981.

N. Sato and S. Kokubun. Interaction between ELF-VLF emissions and magnetic pulsations: Quasiperiodic ELF-VLF emissions associated with Pc 3â€“4 magnetic pulsations and their geomagnetic conjugacy. *J. Geophys. Res.*, 85(A1):101–113, 1980.

N. Sato, K. Hayashi, S. Kokubun, T. Oguti, and H. Fukunishi. Relationships between quasiperiodic VLF emission and geomagnetic pulsation. *J. Atmos. Sol. Terr. Phys*, 36:1515–1526, 1974.

S. S. Sazhin and M. Hayakawa. Periodic and quasiperiodic VLF emissions. *J. Atmos. Terr. Phys.*, 56:735–753, 1994.

E. J. Smith and J. H. Wolfe. Observations of interaction regions and corotating shocks between one and five AU: Pioneers 10 and 11. *Geophys. Res. Lett.*, 3(3):137–140, 1976.

E. Thébault, C. C. Finlay, C. D. Beggan, P. Alken, J. Aubert, O. Barrois, F. Bertrand, T. Bondar, A. Boness, and L. Brocco et al. International geomagnetic reference field: the 12th generation. *Earth Planet Sp.*, 67(1):79, 2015.

E. E. Titova, B. V. Kozelov, A. G. Demekhov, J. Manninen, O. Santolík, C. A. Kletzing, and G. Reeves. Identification of the source of quasiperiodic VLF emissions using ground-based and Van Allen Probes satellite observations. *Geophys. Res. Lett.*, 42:6137–6145, 2015.

M. Tixier and N. Cornilleau-Wehrlin. How are the VLF quasiperiodic emissions controlled by harmonics of field line oscillations? The results of a comparison between ground and GEOS satellites measurements. *J. Geophys. Res.*, 91(A6):6899–6919, 1986.

N. A. Tsyganenko. A magnetospheric magnetic field model with a warped tail current sheet. *Planet. Space Sci.*, 37(1):5–20, 1989.

Publications Appended to the Thesis

A1 Bezděková, B., F. Němec, M. Parrot, O. Santolík, O. Kruparova, Magnetospheric line radiation: 6.5 years of observations by the DEMETER spacecraft *J. Geophys. Res. Space Phys.*, 120 (11): 9442–9456, 2015. doi:10.1002/2015JA021246

A2 Němec, F., B. Bezděková, J. Manninen, M. Parrot, O. Santolík, M. Hayosh, T. Turunen, Conjugate observations of a remarkable quasiperiodic event by the low-altitude DEMETER spacecraft and ground-based instruments *J. Geophys. Res. Space Phys.*, 121 (9): 8790–8803, 2016. doi:10.1002/2016JA022968

A3 Bezděková B., F. Němec, M. Parrot, O. Santolík, V. Krupař, O. Kruparova, Influence of Interplanetary Shocks on ELF/VLF Waves Observed in the Earth's Magnetosphere, in *WDS'18 Proceedings of Contributed Papers — Physics* (eds. J. Šafránková and J. Pavlů), Prague, Matfyzpress, pp. 85–92, 2018.

A4 Němec, F., G. B. Hospodarsky, B. Bezděková, A. G. Demekhov, D. L. Pasmanik, O. Santolík, W. S. Kurth, D. P. Hartley, Quasiperiodic Whistler Mode Emissions Observed by the Van Allen Probes Spacecraft *J. Geophys. Res. Space Phys.*, 123 (11): 8969–8982, 2018. doi:10.1029/2018JA026058

A5 Bezděková, B., F. Němec, M. Parrot, M. Hajoš, J. Záhlava, O. Santolík, Dependence of Properties of Magnetospheric Line Radiation and Quasiperiodic Emissions on Solar Wind Parameters and Geomagnetic Activity *J. Geophys. Res. Space Phys.*, 124 (4): 2552–2568, 2019. doi:10.1029/2018JA026378

A6 Bezděková B., F. Němec, J. Manninen, G. B. Hospodarsky, O. Santolík, W. S. Kurth, D. P. Hartley, Simultaneous Observations of Quasiperiodic Emissions by Spacecraft and Ground-based Instruments, in *WDS'19 Proceedings of Contributed Papers — Physics* (eds. J. Šafránková and J. Pavlů), Prague, Matfyzpress, pp. 106–113, 2019.

A7 Bezděková, B., F. Němec, J. Manninen, G. B. Hospodarsky, O. Santolík, W. S. Kurth, D. P. Hartley, Conjugate Observations of Quasiperiodic Emissions by the Van Allen Probes Spacecraft and Ground-Based Station Kannuslehto *J. Geophys. Res. Space Phys.*, 125 (6): Art. No. e2020JA027793, 2020. doi:10.1029/2020JA027793